Biomedicine & Pharmacotherapy 153 (2022) 113528

Contents lists available at ScienceDirect

Biomedicine & Pharmacotherapy

journal homepage: www.elsevier.com/locate/biopha

Oral sodium butyrate supplementation ameliorates paclitaxel-induced behavioral and intestinal dysfunction

C. Cristiano [a,d,*,1], M. Cuozzo [a,1], L. Coretti [a,d], F.M. Liguori [a], F. Cimmino [c], L. Turco [a,b], C. Avagliano [a], G. Aviello [a], M.P. Mollica [c,d], F. Lembo [a,d], R. Russo [a,d]

[a] Department of Pharmacy, University of Naples Federico II, Italy
[b] Department of Experimental Medicine, University of Campania "Luigi Vanvitelli", Italy
[c] Department of Biology, University of Naples Federico II, Italy
[d] Task Force on Microbiota Studies University "Federico II" of Naples, Napoli, Italy

ARTICLE INFO

Keywords:
Chemotherapeutics
Depression
Neuroinflammation
Gut barrier integrity
Microbiota

Chemical compounds studied in this article:
Paclitaxel (PubChem CID: 36314)
Sodium butyrate (PubChem CID: 5222465)

ABSTRACT

Paclitaxel (PTX) is one of the most broadly used chemotherapeutic agents for the treatment of several tumor types including ovarian, breast, and non-small cell lung cancer. However, its use is limited by debilitating side effects, involving both gastrointestinal and behavioral dysfunctions. Due to growing evidence showing a link between impaired gut function and chemotherapy-associated behavioral changes, the aim of this study was to identify a novel therapeutic approach to manage PTX-induced gut and brain comorbidities.

Mice were pre-treated with sodium butyrate (BuNa) for 30 days before receiving PTX. After 14 days, mice underwent to behavioral analysis and biochemical investigations of gut barrier integrity and microbiota composition. Paired evaluations of gut functions revealed that the treatment with BuNa restored PTX-induced altered gut barrier integrity, microbiota composition and food intake suggesting a gut-to-brain communication. The treatment with BuNa also ameliorated depressive- and anxiety-like behaviors induced by PTX in mice, and these effects were associated with neuroprotective and anti-inflammatory outcomes. These results propose that diet supplementation with this safe postbiotic might be considered when managing PTX-induced central side effects during cancer therapy.

1. Introduction

Patients receiving chemotherapy often experience mood disorders, i.e. approx. 58 % of oncological patients have depression, while 11% experience anxiety attacks [1–3]. These disorders can worsen and lead to longer periods of hospitalization interfering with the success of the therapy [1–5]. Chemotherapy-induced mood disorders and cognitive impairment fall under what is colloquially known as "chemo-brain" or "chemo-fog" and are characterized by several deficits including memory, learning, attention, concentration, executive functions, and visuo-spatial skills [6–9]. A widely supported theory hypothesizes that chemotherapy produces peripheral inflammation that reaching the brain causes neuroinflammation and brain dysfuntions [4–10].

Although there are several chemotherapeutic agents for different types of cancer, only few of them have been studied for their behavioral side effects and possible biological mechanisms involved. Among these, paclitaxel (PTX) is a microtubule-stabilizing agent used to treat primarily solid tumors such as breast, ovarian, and non-small cell lung cancer [11]. Although PTX is lipophilic, it penetrates the blood-brain barrier (BBB) poorly and is rapidly removed from the central nervous system (CNS) [12]; however, despite its low BBB penetration, cognitive and mood symptoms during PTX treatment have been documented

Abbreviations: PTX, paclitaxel; BuNa, sodium butyrate; BBB, blood-brain barrier; CNS, central nervous system; BDNF, brain derived neurotrophic factor; CIPN, paclitaxel-induced peripheral neuropathy; SCFAs, short-chain fatty acids; IL-6, interleukin-6; IL-8, interleukin-8; TNF-α, tumor necrosis factor-α; IL-1β, interleukin-1β; Il-10, interleukin-10; LPS, lipopolysaccharide; Gapdh, glyceraldehyde 3-phosphate dehydrogenase; TST, tail suspension test; FST, forced swimming test; EPM, elevated plus-maze; LDB, light–dark box; CREB, cAMP response element-binding protein; TrkB, tropomyosin receptor kinase B; ZO-1, zonuline-1; Ocln, occludin; GC-MS, gas-chromatography mass spectrometry; FITC-dextran, fluorescein isothiocyanate-labeled dextran.

* Corresponding author at: Department of Pharmacy, University of Naples Federico II, Italy.
E-mail address: claudia.cristiano@unina.it (C. Cristiano).
[1] These authors contributed equally to this work.

https://doi.org/10.1016/j.biopha.2022.113528
Received 29 June 2022; Received in revised form 4 August 2022; Accepted 8 August 2022
Available online 13 August 2022

[13–15] and can lasting for 6 months after its suspension [16]. Interestingly, within the CNS PTX concentrates mainly in the hippocampus and partially in neocortex [17]. The hippocampus is a brain area involved in learning and memory consolidation, but also in neurogenesis [18], whose destruction may be implicated in cognitive impairment and mood disorders [19,20]. Among neurogenesis factors, brain-derived neurotrophic factor (BDNF) is important for neuronal survival and repair [21–23] and its levels increase when there is a neuroprotective effect, such as augmented neurogenesis mediated by antidepressant medications. Importantly, BDNF also plays a protective role in PTX-induced peripheral neuropathy (CIPN) [24,25]. Neurogenesis is normally attenuated by acute or chronic inflammation present in PTX-treated patients. Clinical studies have reported increased circulating levels of interleukin (IL)-6, IL-8 and IFN-γ in patients treated with PTX [26,27]. These cytokines may cross the BBB and trigger neuroinflammation [28] by mediated by tumor necrosis factor-α (TNF-α), IL-1β and IL-6 [29–31]. However, how PTX-induced peripheral inflammation impinges hippocampal function is still unclear [29–32]. In addition to cognitive and mood disorder, PTX is also known to induce chemotherapy-induced peripheral neuropathy (CIPN) as well as gastrointestinal symptoms [33–37], two other manifestations often related to depression and anxiety [38]. The gastrointestinal symptoms have its main origin from chemotherapy-induced intestinal microbial dysbiosis, characterized by an imbalanced proportion between beneficial and pathogenic bacteria, possibly explaining PTX's central effects through a gut-brain axis [39–44].

Although this link has not been shown in patients undergoing treatment with chemotherapy, it is nevertheless true that chemotherapy including PTX alters the fecal bacterial communities [45,46], and therefore this relationship is plausible. Confirming this, the study by Loman et al. [47], reveals the relationship among behavior, central and peripheral immune activation, and microbiota in PTX-treated mice.

There is a critical need to better investigate the relationship between PTX-induced depressive and gastrointestinal symptoms and the role of gut microbiota in modulating host response following PTX treatment, in order to identify new strategies to counteract its detrimental effects on both gut and brain functions.

Short-chain fatty acids (SCFAs), i.e. acetate, propionate and butyrate, are produced by the microbial fermentation of dietary fibers in the intestine and represent 86 % of total SCFAs [48]. They show multiple beneficial effects on human health. Indeed, diet supplements of SCFAs restores eubiosis, attenuates inflammation, maintains barrier function, promotes antitumor effects, and mucosal repair mechanisms altered by cancer treatments [49,50]. Among SCFAs, butyrate exerts several beneficial effects with different mechanisms of action, including a potent regulation of gene expression [51]. Butyrate maintains gut homeostasis by improving inflammation [52,53], oxidative status [54] and epithelial barrier defense [55]. In the CNS, butyrate crosses the BBB and has antidepressant and anti-inflammatory effects when administered intraperitoneally [56].

Previous studies have shown that following chemotherapy, patients have low levels of SCFA-producing bacteria in their gut microbiota and decreased SCFAs concentration in fecal samples, conditions often accompanied by impaired barrier function [37–49]. Thus, the aim of this study was to investigate the effects of preventive administration of sodium butyrate (BuNa) in mice treated with one cycle of PTX on gut function and microbiota composition and, importantly correlate them with the assessment of anxiety- and depressive-like behaviors as well as central neuroinflammation.

2. Materials and methods

2.1. Animals

CD1 male mice (25–30 g Charles Rivers-Italy) were housed in a temperature-controlled (22 ± 1 °C) environment in a 12 h light/dark cycle with ad libitum food and water, in the animal care facility at the Department of Pharmacy of the University of Naples Federico II, Italy. All behavioral tests were performed between 09:00 and 14:00 h. Animal care and manipulations were carried out in conformity with International and National law and policies (EU Directive 2010/63/EU for animal experiments, ARRIVE guidelines, and the Basel declaration including the 3R concept). The procedures reported here were approved by the Institutional Committee on the Ethics of Animal Experiments (CVS) of the University of Naples Federico II (No. 595/2019-PR, approved 30 July 2019).

2.2. Experimental groups and procedures

Study protocol for PTX and BuNa treatments is reported in Fig. 1. Briefly, four groups of n = 8 mice each were set. BuNa was given orally for 44 days in daily drinking water (control group received water only). After 30 days, mice were randomly divided into two groups, one receiving PTX and the other one vehicle (5 % DMSO + 40 % PEG 300 + 5 % Tween 80 + ddH2O), both injected intraperitoneally (i.p.). Animals received PTX or vehicle treatments every other day for a week (days 1, 3, 5, and 7). Seven days after the last injection, mice were subjected to behavioral tests and after euthanasia, blood and tissues (i.e. colon and hippocampus) were collected for ex vivo analysis.

The four groups are indicated as follow:

- **Vehicle:** mice receiving drinking water for 44 days and, subsequently vehicle (100 ul/mouse) i.p. at day 1, 3, 5, and 7.
- **BuNa:** mice receiving BuNa dissolved in drinking water (0.23 mg/ml) for 44 days and subsequently vehicle (ul/mouse) i.p. at day 1, 3, 5, and 7.
- **PTX:** mice receiving drinking water for 44 days and, subsequently paclitaxel (8 mg/kg, 100 ul/mouse) i.p. at day 1, 3, 5, and 7.
- **BuNa+PTX:** mice receiving BuNa dissolved in drinking water (0.23 mg/ml) for 44 days and subsequently paclitaxel (8 mg/kg, 100 ul/mouse) i.p. at day 1, 3, 5, and 7.

Individually body weight and home-cage food intake (n = 2 mice per cage) were recorded from day 0 to 14 and reported every 48 h as a percent change from baseline (n = 6/group).

2.3. Drug treatment

Paclitaxel (PTX, Cat#S1150 Selleckchem, USA) was dissolved in a solution made up of 5 % DMSO + 40 % PEG 300 + 5 % Tween 80 +ddH2O according to manufacture guideline. PTX (8 mg/kg) or vehicle (both in 100 μl/mouse) were injected i.p. every other day for a total of 4 doses (days 1, 3, 5, and 7, as shown in Fig. 1), according Toma et al. [57].

Sodium butyrate (BuNa) (Cat#303410 Sigma-Aldrich, Italy) was dissolved in daily drinking water at the concentration of 0.23 mg/ml, selected from previous studies [58]. Fresh bottles were changed daily, and liquid consumption quantified. Assuming that mice drink an average of 4 ml/day, BuNa-treated water resulting in an estimated dose of 30 mg/kg/day.

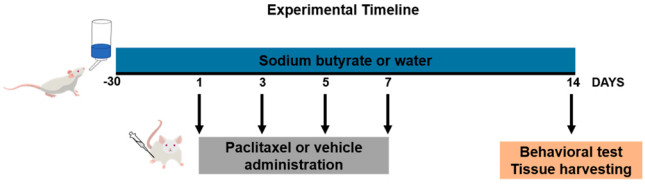

Fig. 1. Schematics showing the experimental timeline for both sodium butyrate and paclitaxel administrations and behavioral tests/tissue harvesting.

2.4. Behavioral tests

2.4.1. Depressive-like behavior

2.4.1.1. Tail suspension test (TST). Each mouse was suspended by the tail 30–40 cm above the floor using adhesive tape placed approximately 2 cm from the tip of the tail for a 6 min-period. Immobility time, expressed in seconds, was monitored during the test using a timer. Mice were defined immobile when they did not show any body movement, hung passively and motionless during suspension.

2.4.1.2. Forced swimming test (FST). Each mouse was placed in a cylinder (30 cm × 45 cm) filled with water at a temperature of 27 °C for 10 min. Immobility time, expressed in seconds, was monitored during the test using a timer. Mice were considered immobile when they remained floated and motionless and making only movements necessary to keep their head above the water. After the test, mice were allowed to dry and return to their home cage; cylinders were emptied and rinsed at the end of each test.

2.4.2. Anxiety-like behavior

2.4.2.1. Elevated plus-maze (EPM). The maze consisted of two opposite open and closed arms (35 cm × 7 cm) elevated 50 cm from the floor. The animals were individually placed in the center with their heads facing toward a closed arm and allowed to move freely. Each mouse was recorded using a camera capture and analyzed using a video tracking software (Any-maze, Stoelting, Wood Dale, IL, USA). We analyzed the number of entries in the open-arm choice during a period of 5 min.

2.4.2.2. Light–dark box (LDB). The apparatus consisted of two equally sized compartments (60 cm × 30 cm × 30 cm) connected by a door: one covered as dark compartment and the other one opened and brighted as light compartment. Each mouse was individually placed in the light compartment and allowed to freely explore both boxes over a period of 10 min. The time spent in the light compartment was recorded using a timer.

2.4.2.3. Novelty suppressed feeding (NSF). This test assesses rodent's stress-induced anxiety by measuring its latency to approach and eat a familiar food in a novel environment. Briefly, mice were fasted for 24 h and then placed individually in a cage and allowed to access to an unused, pre-weighed food pellet. The latency to eat expressed in seconds, defined as the mouse sitting on its haunches and biting the pellet with the use of forepaws, was recorded using a timer.

2.5. Fecal SCFAs extraction

Fecal samples were collected after defecation and stored at − 20 °C until analyzed. Briefly, 100 mg of fecal samples were mixed with 200 μl of sterile water and homogenized for 3 min, then centrifuged for 30 min at 12,000 × *g* at room temperature (RT). The supernatants (solubilized feces) were filtered and transferred into a new tube, where 20 μl of 85 % (w/v) phosphoric acid (H_3PO_4) was added and mixed for 5 min. For SCFA extraction, anhydrous diethyl ether (DE) was added to the acidified fecal homogenate samples (1:1, v/v), vortexed and centrifuged for 30 min at 12,000 × *g* at RT. The DE layer (containing SCFAs) was transferred into a new glass tube, where sodium sulfate anhydrous was added in order to remove the residual water. Finally, organic phase was placed in a new glass tube for gas-chromatography mass spectrometry (GC-MS) analysis. For each SCFA, a standard curve (10–200 μg/ml) was generated at the beginning of the run. A blank solvent (DE) was injected between every sample to ensure no memory effects.

2.6. Gas-chromatography mass spectrometry (GC/MS) analysis

The GC column was an Agilent 122-7032ui (DB-WAX-U, Agilent Technologies, Santa Clara, California, USA) of 30 m, internal diameter of 0.25 mm, and film thickness of 0.25 μm. The GC was programmed to achieve the following run parameters: the initial column temperature was set at 90 °C, hold of 2 min, and then increased to 100 °C at a rate of 2 °C/min, hold of 10 min, finally ramp of 5 °C/min up to a final temperature of 110 °C for a total run time of 21 min, gas flow of 70 ml min^{-1} splitless to maintain 12.67 p.s.i. column head pressure, and septum purge of 2.0 ml min^{-1}. Helium was the carrier gas (1.5 ml min^{-1} constant). Parameters of mass spectrometer were: source at 230 °C and MS Quad at 150 °C.

2.7. Ex vivo experiments

At day 14, mice were euthanized, and bloods, hippocampi and colons were collected for the further analyzes, as follows.

2.7.1. Determination of serum and hippocampal markers of inflammation

Blood was collected by cardiac puncture and serum obtained by centrifugation at 1500g at 4 °C for 15 min and then stored at − 80 °C until use. Serum TNF-α, Il-1β, Il-6, Il-10 and lipopolysaccharide (LPS) levels (ng/ml) were measured by ELISA (BD Pharmingen), according to the manufacturer's instructions. At the same time hippocampi were collected and TNF-α, IL-1β, IL-6, and IL-10 levels were measured by real time (RT)-PCR. For RT-PCR, total RNA was extracted from brain areas using TRIzol Reagent (Bio-Rad Laboratories) according to the manufacturer's instructions. cDNA from 4 μg total RNA was retro-transcribed using a reverse transcription kit (NucleoSpin®, MACHEREY-NAGEL GmbH & Co, Düren, Germany). RT-PCR reactions were performed using Bio-Rad CFX96 PCR System and relative software (Bio-Rad Laboratories). Mouse primers for *Tnf*, *Il1b*, *Il6*, and *Il10* were purchased from Qiagen (Hilden, Germany). Glyceraldehyde 3-phosphate dehydrogenase (*Gapdh*) was used as housekeeping gene for normalization. Data were expressed using the ΔΔCT method.

2.8. Western blot analysis

Colonic and hippocampal tissues were homogenized in ice-cold lysis buffer (10 mM Tris–HCl, 20 mM, pH 7.5, 10 mM NaF, 150 mM NaCl, 1 % Nonidet P-40, 1 mM phenylmethylsulphonylfluoride, 1 mM Na_3VO_4, leupeptin, and trypsin inhibitor 10 μg/ml) and total protein lysates underwent SDS-PAGE electrophoresis followed by transfer on nitrocellulose membranes. Specific binding sites were blocked with 3% nonfat dried milk (Bio-Rad, Hercules, CA, USA) for 45 min at room temperature, and them membranes were incubated overnight at 4 °C in the presence of the following primary antibodies in the same blocking solution: rabbit polyclonal anti-phospho-cAMP response element-binding protein (CREB) or anti-CREB (dilution 1:1000; Cat#9196, and Cat#4820, respectively; Cell Signaling Technology, Danvers, MA, USA), anti-BDNF (dilution 1:1000; Cat#ab108319; Abcam), anti-tropomyosin receptor kinase B (TrkB, dilution 1:1000; Cat#4603; Cell signaling) and anti-zonuline-1 (ZO-1; dilution 1:1000, Cat#40–2300 Invitrogen, Milan, Italy). Subsequently, the membranes were incubated with the appropriate secondary antibody (Jackson ImmunoResearch, West Grove, PA, USA) for 1 h at room temperature. The antibody-reactive bands were revealed by chemiluminescence using a ChemiDoc imaging instrument (Bio-Rad, Segrate, Italy). Immunoblotting for β-actin (1:5000; Cat#A5441; Sigma-Aldrich, Milan, Italy) was used for normalization.

2.9. Measurement of gut permeability in vivo

In another set of experiments, mice were fasted for 12 h and then gavaged with 4-kDa fluorescein isothiocyanate-labeled dextran (FITC-dextran; TdB Consultancy AB, Uppsala, Sweden) diluted in water

(500 mg/kg, 125 mg/ml). After 4 h, blood (500 μl) was collected and FITC-dextran concentration in plasma was determined by spectrofluorimetry (excitation wavelength: 485 nm and emission wavelength: 535 nm; HTS-7000 Plus-plate-reader, Perkin Elmer), as previously described [59].

2.10. Gut microbiota sequencing and data analysis

Microbiota analysis was carried out on cecal samples of a subset of six mice per group by sequencing the V3–V4 regions of the 16 S rRNA gene as previously described [60]. Metagenomic analysis was achieved using the Quantitative Insights Into Microbial Ecology (QIIME2, version 2021.4) [61]. Briefly, demultiplexed paired end reads from Miseq were processed and quality filtered (i.e. filtered, dereplicated, denoised, merged, and assessed for chimeras) to produce amplicon sequence variants (ASVs) using DADA2 pipeline [62]. To obtain a superior classification precision, taxonomy was assigned using the Weighted Taxonomic Classifier "Greengenes 13_8 99 % OTUs from 515F/806R region of sequences" [63–65]. Moreover, to increase the species taxonomic level resolution, the representative fasta sequence of each ASV from DADA2 was aligned to the rRNA/ITs BLAST database using blastn [66]: resulting hits were sorted first by e-value, then bitscore and the taxonomy of the highest scoring sequence was reported. Samples were normalized using a maximum depth of 25,567 sequences/sample applying sequence rarefaction procedure. The intra- and inter-group diversity of bacterial communities were examined using alpha (Good's coverage, Shannon's diversity index, and Observed features) and beta diversity (unweighted and weighted UniFrac distances) metrics; statistical group significance of alpha and beta diversity indexes was assessed with QIIME2 plugins using the Kruskal–Wallis test and Analysis of similarities (ANOSIM) method, respectively. Furthermore, the linear discriminant analysis effect size (LEfSe) method (https://huttenhower.sph.harvard.edu/galaxy) [67] was employed to identify key ASVs that discriminated between groups based on their relative abundance (LEfSe; $p < 0.05$ by Kruskal–Wallis test, $p < 0.05$ by pairwise Wilcoxon test and logarithmic LDA score of 2.0); key features were represented in a heatmap with clustering on the feature axis [68].

2.11. Statistical analysis

Sample size was determined by power analysis based on effect sizes by using Gpower software. The data and statistical analysis comply with the recommendations on experimental design and analysis in pharmacology [69]. The statistical analyses were performed using Prism 9 Graphpad software (GraphPad Software Inc., San Diego, CA, USA) and all data are presented as mean ± SEM. The significant of differences among groups was determined by one or two-way repeated measurements ANOVA followed by Tukey's post hoc multiple comparison test. Data are represented as mean ± standard error mean (SEM). A $p < 0.05$ was considered statistically significant for all tests.

3. Results

3.1. Effect of BuNa on PTX-induced alterations in fecal short chain fatty acids

Levels of SCFA (i.e. acetic, propionic and butyric acids) were determined after 14-day PTX treatment. PTX selectively reduced fecal levels of butyric acid (*$p < 0.05$; Fig. 2A), while did not have any effect on acetic and propionic acid. The effect of PTX on butyric acid suggested a less preserved gut homeostasis [70]. The treatment with BuNa significantly increased fecal levels of butyric acid in both control (***$p < 0.001$; Fig. 2A) and PTX-treated mice (**$p < 0.01$; Fig. 2A), while it was able to increase only the fecal level of acetic acid in both control (*$p < 0.05$) and PTX-treated mice (*$p < 0.05$; Fig. 2B). Levels of propionic acid remained unchanged.

3.2. Effect of BuNa on PTX-induced alterations in microbiota composition

To investigate the impact of PTX and the pre-treatment with BuNa on gut microbiota composition we profiled the bacterial communities in the ceca of all groups using 16 S rRNA sequencing. After processing, a total 984,163 high quality reads were acquired with an average number of 41,006.8 reads/sample (minimum frequency of 25,567 reads) clustered into 5594 Amplicon Sequence Variants (ASVs; mean Good's Coverage over 99 %). Unweighted and weighted beta diversity analyses showed a clear difference in overall microbiota composition among all groups (Fig. 3A and B). In both PCoA plots, vehicle and PTX groups were diametrically opposed, indicating a strong difference in bacterial assortment between the two microbial communities (ANOSIM $R = 0.737$ and $R = 0.804$ with $p < 0.001$ for unweighted and weighted comparison of dissimilarities, respectively). BuNa prolonged treatment strongly affected the structure of bacterial populations compared to vehicle and PTX groups. Specifically, protracted treatment with BuNa in PTX group clearly impacted on microbial communities by reducing the taxonomic complexity and increasing the dissimilarity in relative abundance of shared species with respect to vehicle (Fig. 3A and B). The microbiota profile of PTX-treated mice was characterized by a significant imbalance in the Bacteroidetes/Firmicutes ratio compared to vehicle (**$p < 0.01$), being the treatment with BuNa able to restore the *phyla* assortment to control levels mainly due to Bacteroidetes reduction in PTX treated mice (*$p < 0.05$), without any effect per se (Fig. 3C). LEfSe analysis at the amplicon sequence variants (ASV) level, taxonomically implemented using the BLAST NCBI Database, identified 197 ASVs significantly changed among groups (LDA score >2). Fig. 3D highlights a phylogenetic clustering of the ASVs with higher discriminant power (LDA score > 3) among the three principal groups. While ASVs classified as *Alistipes senegalensis* characterized the microbiota of vehicle group, 2 ASVs belonging to *Alistipes massiliensis*, 2 classified as *Prevotella stercorea* and 1 of *Odoribacter splanchnicus* marked PTX bacterial communities; pre-exposure with BuNa followed by the treatment with PTX reshaped the

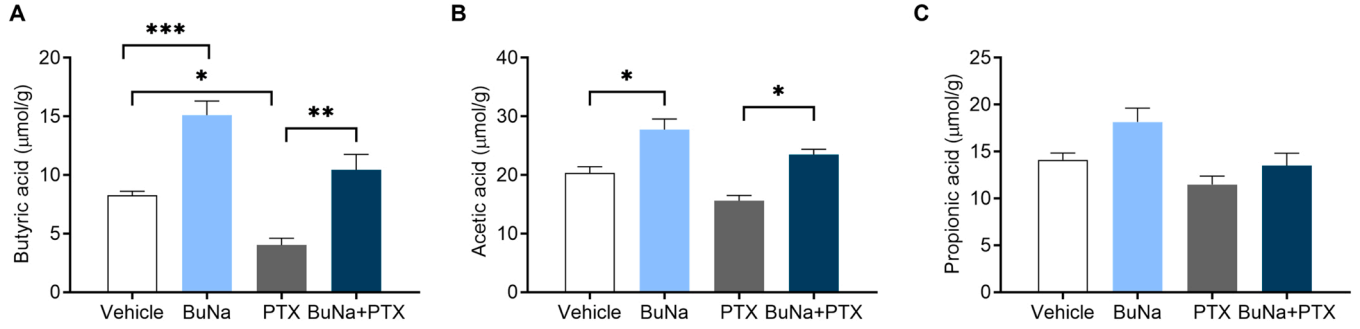

Fig. 2. SCFA levels in fecal sample. Butyric acid (A), acetic acid (B) and propionic acid (C) levels in fecal samples. Results are shown as mean ± SEM ($n = 5$). Differences have been evaluated by ANOVA followed by Tukey's post hoc test for multiple comparisons, *$p < 0.05$, **$p < 0.01$, ***$p < 0.001$ versus relative control.

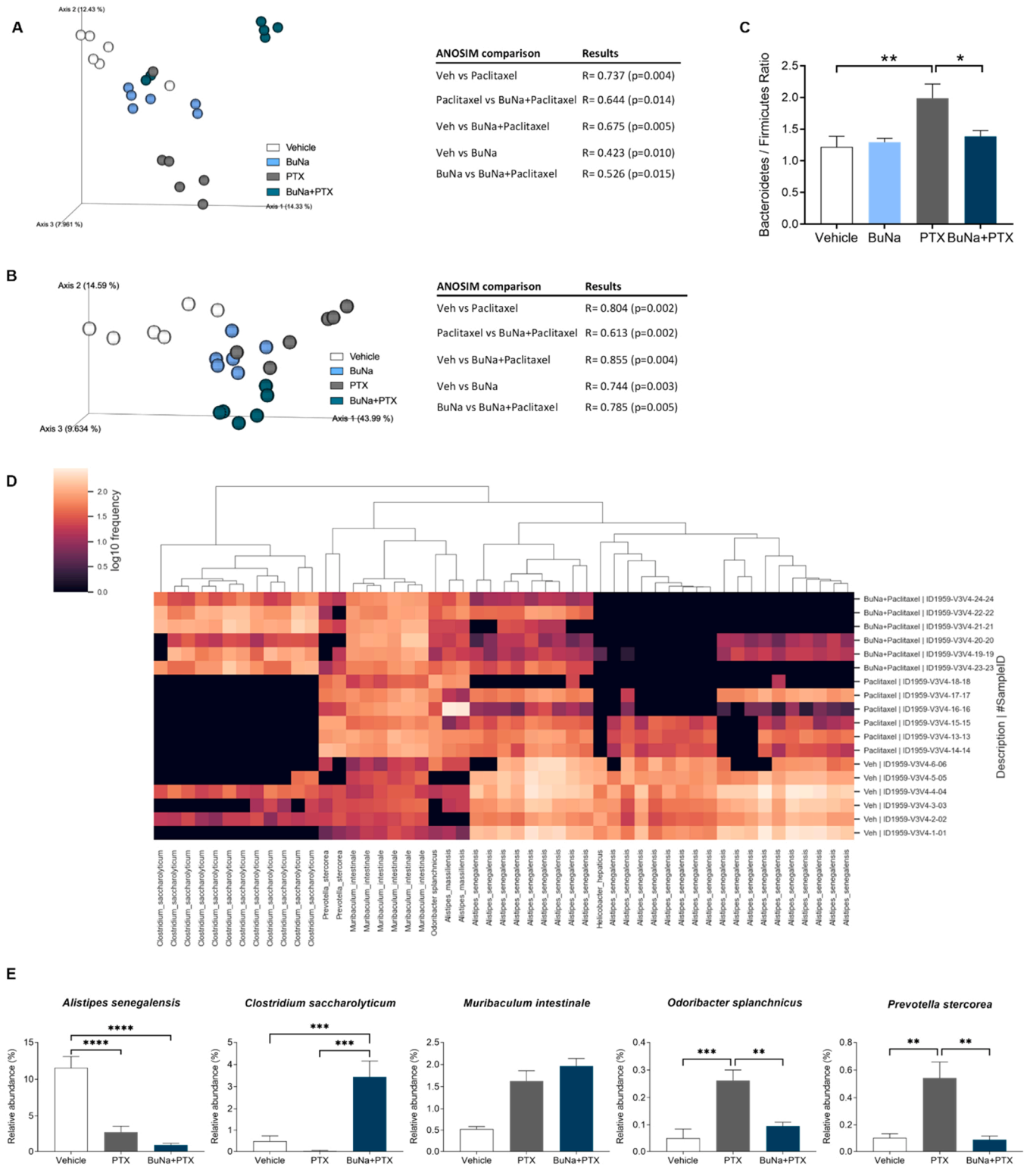

Fig. 3. Effects of BuNa pre-treatment on PTX-induced gut dysbiosis. Principal coordinate analysis (PCoA) plots, based on unweighted and weighted UniFrac distance matrix, respectively (25,567 sequences/sample) (A, B). On the bottom of the PCoA plot are reported both R statistics and p values of the ANOSIM (Analysis of similarity) statistical method performed with 999 permutations used to detect the statistically significant differences in microbial community composition among the groups. Ratio of Bacteroidetes to Firmicutes (C) in each sample group (mean ± SEM, $^{**}p < 0.01$ and $^{***}p < 0.001$, one-way ANOVA followed by Tukey's post hoc test for multiple comparisons). Heatmap showing the ASVs with higher discriminant power among groups (D) based on linear discriminant analysis (LDA) combined with effect size (LEfSe) algorithm ($p > 0.05$ for both Kruskal–Wallis and pairwise Wilcoxon tests and a cutoff value of LDA score above 3.0); species taxonomic classification of ASVs was performed using BLAST to align each representative ASV sequence to rRNA/ITs BLAST database. Significant differences in relative abundance of key ASVs discriminating bacterial communities collapsed at species level (E) (mean ± SEM; $^{**}p < 0.01$ and $^{***}p < 0.001$, one-way ANOVA followed by Tukey's post hoc test for multiple comparisons).

microbiota composition by increasing 12 and 6 ASVs classified as *Clostridium saccharolyticum* and *Muribaculum intestinale*, respectively. Moreover, comparison of the discriminant ASVs mean abundances collapsed at species level clearly showed that BuNa restored to vehicle levels the abundance of *Odoribacter splanchnicus* and *Prevotella stercorea* (**p < 0.01; Fig. 3E).

3.3. Effect of BuNa on gut permeability and food intake

Considering that PTX mainly affected the balance between Bacteroidetes/Firmicutes and their species assortment, we studied the effects of repeated BuNa administrations on gut permeability and intestinal barrier integrity. We found that PTX-treated mice were characterized by compromised gut epithelial barrier integrity, since a significant increase in plasma levels of FITC-labeled dextran 4 h after its oral gavage was observed in PTX-treated mice (*p < 0.05; Fig. 4A). BuNa administration in PTX-treated mice was able to fully restore (*p < 0.05; Fig. 4A) barrier impairment induced by PTX (Fig. 4). Additional barrier integrity investigation was performed by studying the expression on the key tight junction protein zonulin-1 (ZO-1). Representative images of western blot analysis are reported in Fig. 4B. At the densitometry analysis, PTX-treated mice presented a significant reduction of colonic ZO-1 protein expression compared to vehicle group (Fig. 4B). This effect was fully restored be repeated BuNa administrations in PTX-treated mice (Fig. 4B, *p < 0.05 vs relative control). We further analyzed the effect of BuNa treatment on changes in food intake and body weight caused by PTX. PTX treatment concurrently inhibited body weight gain, more significantly at the beginning of PTX treatment (**p < 0.01; Fig. 4C) and food intake over time (*p < 0.05, **p < 0.01 and ***p < 0.001 versus vehicle; Fig. 4D). Specifically, while vehicle-treated mice gained weight throughout the course of the experiment, PTX-treated mice did not. Repeated BuNa administrations in PTX-treated mice restored body weight and food intake ($^{\#}$ p < 0.5 vs PTX; Fig. 4D). These results were accompanied with an increased of latency to eat in the novelty suppressed feeding test (**p < 0.01; Fig. 4E) decreased by repeated BuNa administrations in PTX-treated mice (*p < 0.05; Fig. 4E).

3.4. Effect of BuNa on PTX-induced increased serum levels of pro-inflammatory markers

A systemic anti-inflammatory effect of BuNa administration in PTX-treated mice was also evaluated by measuring serum levels of TNF-α, IL1β, IL6, LPS and IL-10 using ELISA. Mice treated with PTX showed a significant increase in all pro-inflammatory mediators and as well as an increase in IL-10 levels compared to controls (*p < 0.05 and ****p < 0.0001 versus vehicle; Fig. 5A–D). Repeated BuNa administration in PTX-treated mice reduced the pro-inflammatory signature of PTX-treated mice by reducing TNF-α, IL1β, IL6, and LPS levels (**p < 0.01 and ****p < 0.001 versus PTX, Fig. 5A–D). Although a small trend, the effect of BuNa on IL-10 levels was not significant.

3.5. Effect of BuNa on PTX-induced behavioral impairments

To assess whether PTX had any effect on mood, we investigate depressive- and anxiety-like behaviors. As expected, mice repeatedly treated with PTX showed increased immobility time compared to vehicle-treated mice (**p < 0.01; Fig. 6A) in the TST. These results were recapitulated in the FST as well (*p < 0.05, ****p < 0.0001; Fig. 6B). Repeated BuNa administrations significantly reduced the time of immobility in PTX-treated mice compared to the group receiving PTX only in either the TST (*p < 0.05; Fig. 6A) or the FST (****p < 0.0001; Fig. 6B).

In the LDB test PTX-treated mice showed a significant decreased in the time spent in the light side of the box (***p < 0.0001; Fig. 6C) as well as in the open arms of the EPM (*p < 0.05; Fig. 6D) if compared to vehicle-treated mice. Prolonged BuNa administration in PTX-treated mice significantly increased the time spent in both the light side of LDB (*p < 0.05; Fig. 6C) and in the open arms of the EPM (*p < 0.05: Fig. 6D). Data obtained in the models of anxiety-like behavior were in line with those obtained in depressive-like behavioral models suggesting that the prolonged treatment with BuNa resulted in a protective effect against PTX-induced behavioral changes.

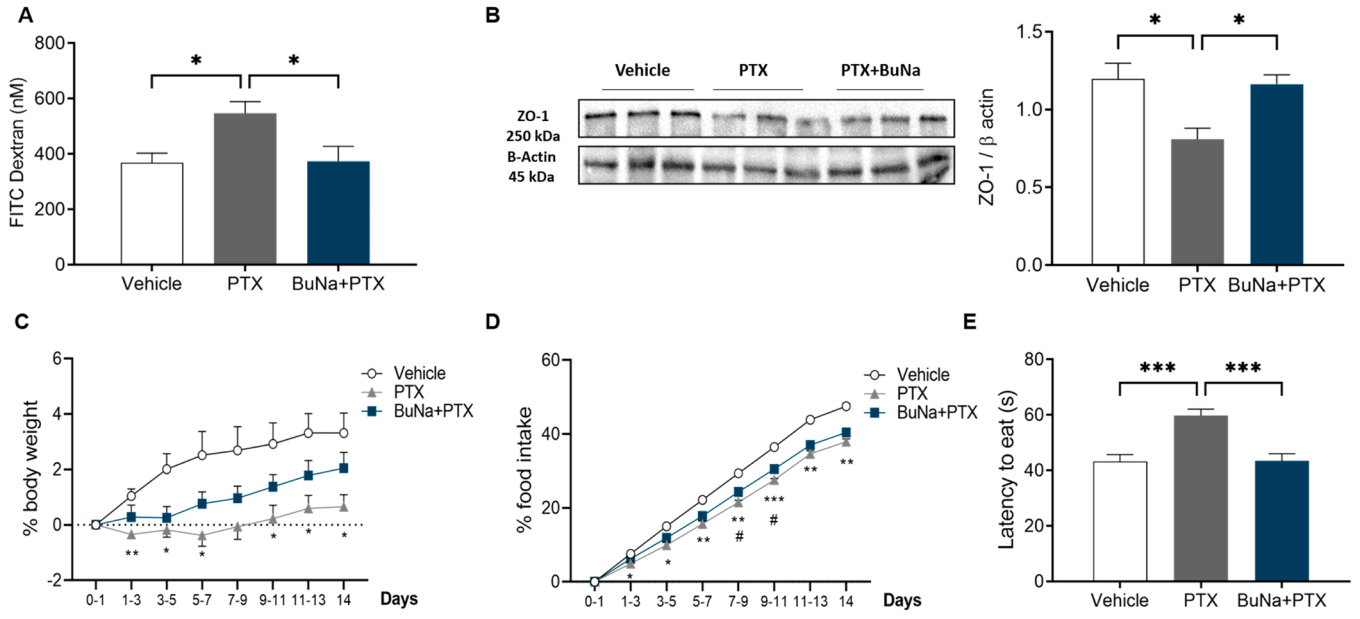

Fig. 4. Effects of BuNa treatment on PTX-induced increased gut barrier permeability. Ex vivo detection of plasma levels of FITC-labeled dextran (A), *p < 0.05 versus relative control (n = 6 per group). Representatives immunoblot image for colonic ZO-1 protein expression (n = 3 per group) and densitometry analysis of ZO-1 (B). (C) % change in body weight (D) % change in food intake relative to baseline. (E) Latency to eat in the novelty suppressed feeding test expressed in seconds. Results are shown as mean ± SEM. Differences were analyzed using ANOVA followed by Tukey's post hoc test for multiple comparisons (*p < 0.05, **p < 0.01 and ***p < 0.001 versus relative control; $^{\#}$p < 0.5 vs PTX group).

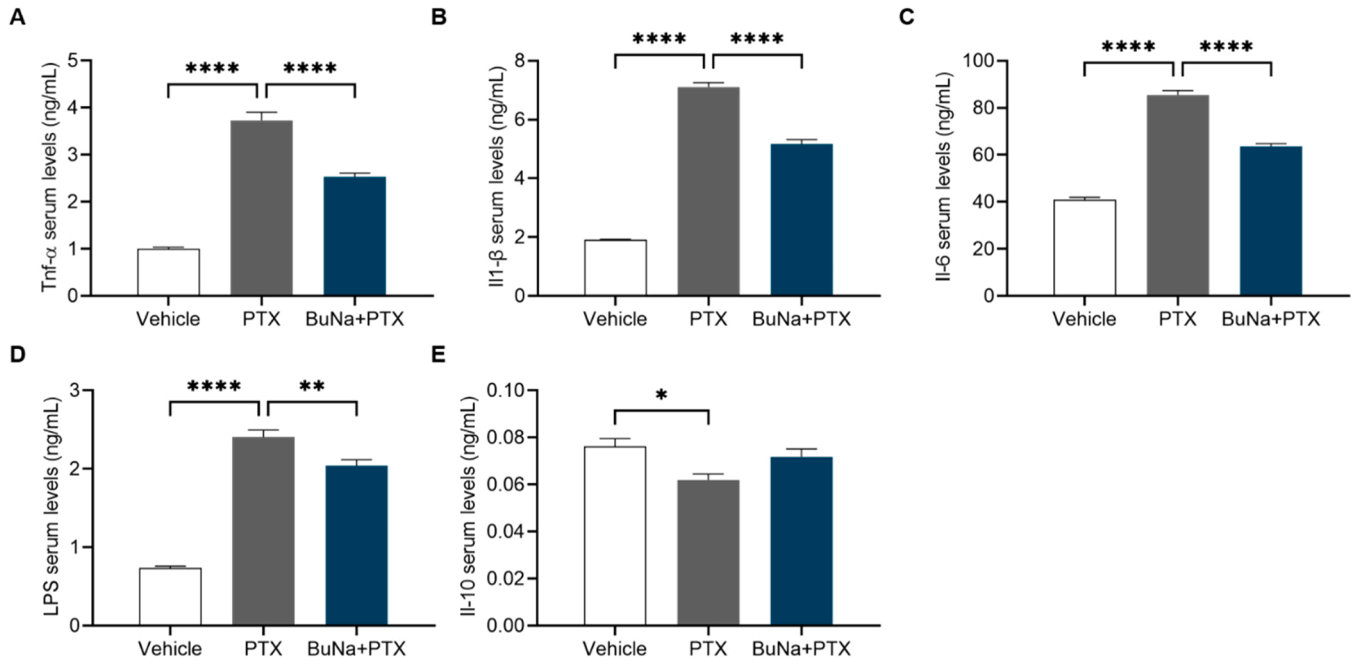

Fig. 5. Effect of BuNa on systemic inflammatory markers. Serum levels of TNF-α (A), IL1β (B), IL6 (C), LPS (D) and IL-10 (E) analyzed by ELISA (n = 5 per group). Results are shown as mean ± SEM. Differences were calculated using ANOVA followed by Tukey's post hoc test for multiple comparisons (*p < 0.05, **p < 0.01 and ****p < 0.0001 versus relative control).

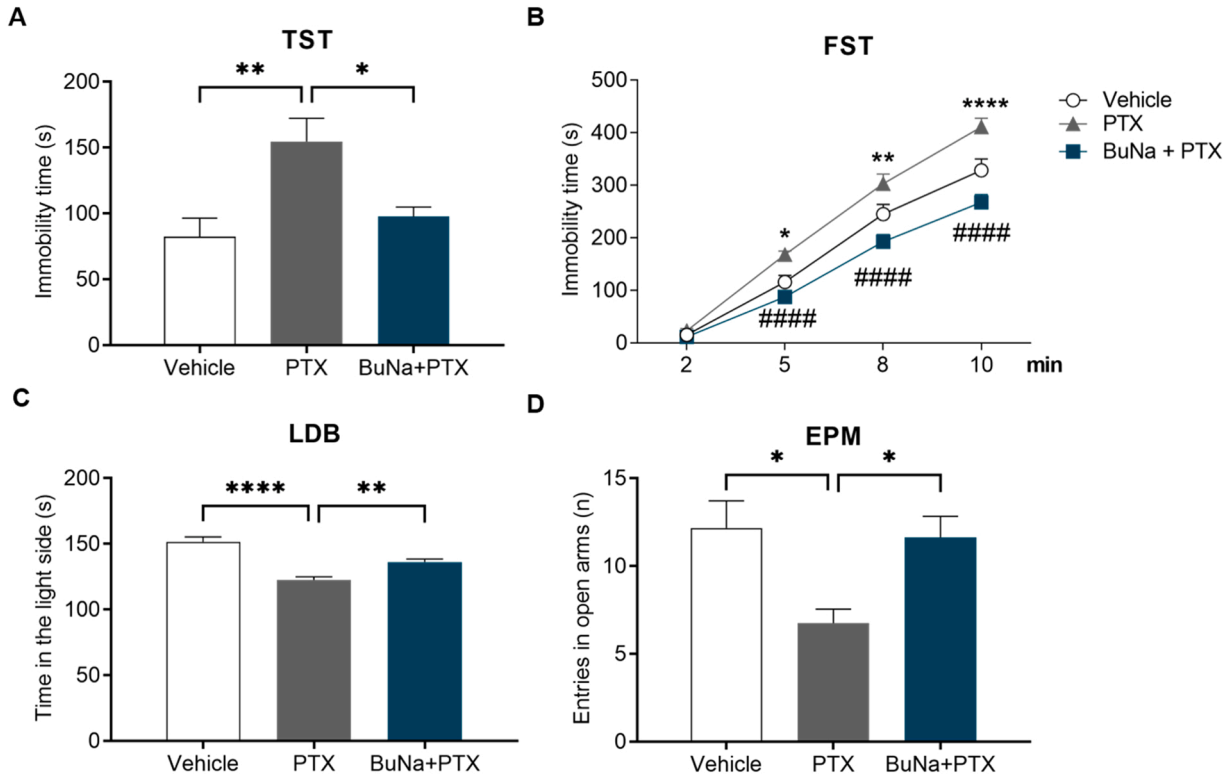

Fig. 6. Depressive- and anxiety-like behavioral tests. Time (in seconds) spent immobile in the tail suspension test (A) and in the forced swimming test (B). In (A) *p < 0.05, and **p < 0.01 versus relative control, while in (B) *p < 0.05, **p < 0.01, ****p < 0.0001 vs vehicle, and $^{\#\#\#\#}$p < 0.0001 versus PTX. Time (in seconds) spent in the light side of the light-dark box (C) and number of entries in the open arms of elevated plus maze test (D) to evaluate anxiety-like behavior. In (C) and (D) *p < 0.05 and ****p < 0.0001 versus relative control. Data are presented as mean ± SEM (n = 8). Differences have been evaluated by ANOVA followed by Tukey's post hoc test for multiple comparisons.

3.6. Effect of BuNa on hippocampal neuroinflammation

Quantitative PCR analyses showed that PTX treatment increased the levels of proinflammatory genes, particularly *Tnf* and *Il1b* in the hippocampi of mice while decreased the levels of *Il10* (**p < 0.01 versus vehicle; Fig. 7A-D). A non-significant trend towards an increase of *Il6* was also observed. Repetitive BuNa administration of PTX-treated mice reduced all pro-inflammatory cytokine gene levels analyzed (i.e. *Tnf*, *Il1b* and *Il6*) while increasing the levels of *Il10* (*p < 0.05, **p < 0.01, and ***p < 0.001 versus PTX; Fig. 7A–D). These data suggested a protective profile of BuNa repeated treatment with regards to hippocampal neuroinflammatory markers.

3.7. BuNa-mediated hippocampal modulation of BDNF, TrkB and CREB protein expression

To delineate how changes in BDNF signaling impact on mouse behavior, we analyzed the protein expression of BDNF and its receptor, tropomyosin receptor kinase B (TrkB) in the hippocampus of mice treated with PTX and BuNa. PTX administration induced a significant loss of BDNF and TrkB receptor expression compared to the vehicle group (*p < 0.05 PTX versus vehicle), while the treatment with BuNa significantly totally or partially restored their expressions (*p < 0.05 and **p < 0.01 versus PTX) (Fig. 8A–B). Although no difference was reported between PTX and vehicle groups in the expression of pCREB/CREB, BuNa administration in PTX-treated mice caused an increase (*p < 0.05) in pCREB/CREB ratio (Fig. 8C).

4. Discussion

In this study we investigated the effect of prolonged oral treatment with postbiotic BuNa on PTX-induced intestinal dysfunction and depression- and anxiety-like behavioral changes paving the way to its potential use in counteracting PTX-associated side effects via modulation of the gut-brain axis.

Several studies have reported that PTX induces mood disorders [12–14], CIPN [24,25], inflammation [42], dysbiosis and microbiota perturbation [33–37]. Noteworthy, a previous study found that pharmacokinetic parameters (i.e., distribution and elimination) of distinct PTX formulations are different in mice and humans. This correlates with a significant species-dependent difference in efficacy and adverse effects, affecting the translatability of the PTX model [71].

To increase our understanding in PTX-induced side effects, the dose of PTX in this study able to induce gut dysbiosis couples with brain dysfunction and behavioral deficits, was chosen on the basis of our previous experiments [72], and other studies [57].

In line with these findings, in our study one cycle of PTX (for a total of four injections) resulted in both intestinal and central effects in mice, including impaired food intake, altered gut barrier and microbiota composition and depression- and anxiety-like symptoms. All these effects were studied in non-tumor bearing mice to exclude the consequences related to tumor growth and focus on the actual contribution of BuNa intake on chemotherapy-induced side effects.

In particular, intestinal alterations induced by PTX included diarrhea, presence of blood in stools, abdominal pain, nausea and colitis, and required pharmacological treatments. This condition may be also

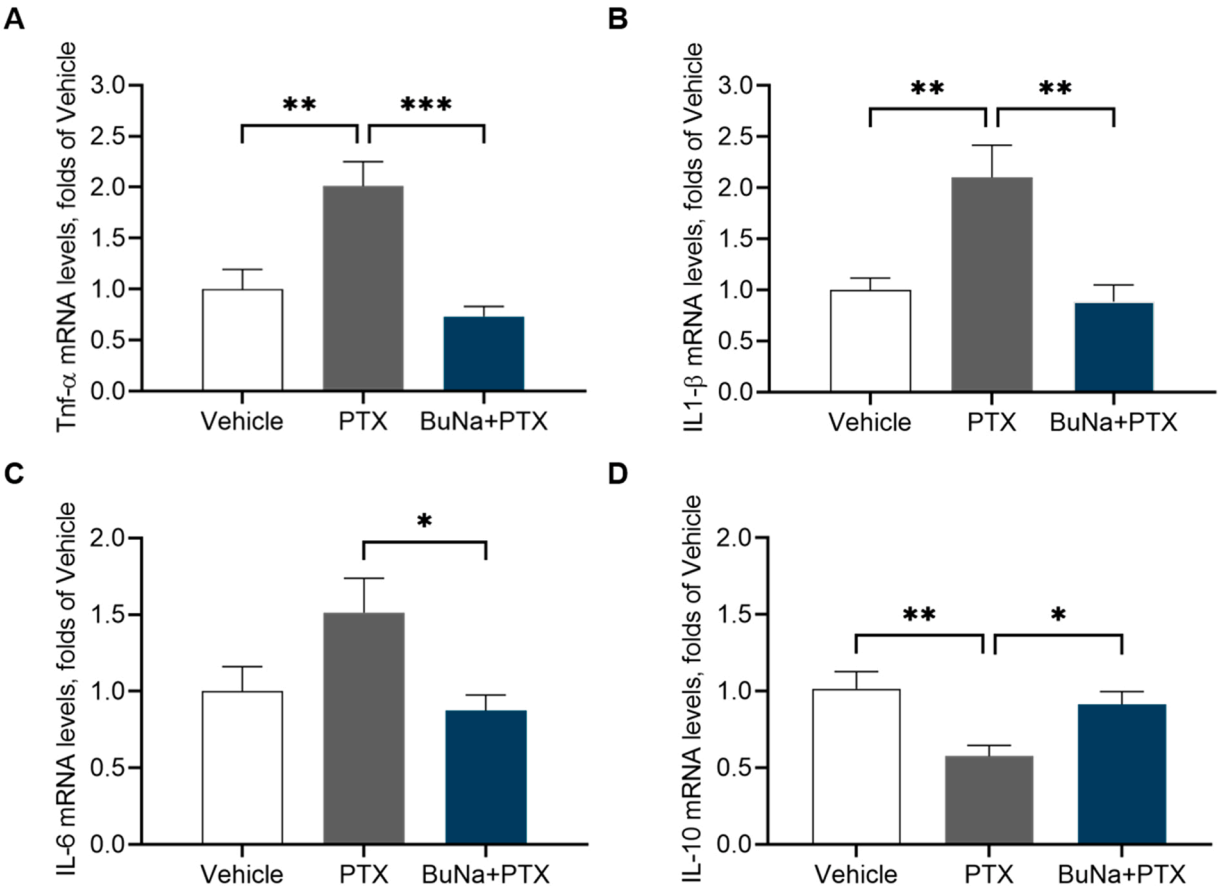

Fig. 7. Hippocampal pro-inflammatory cytokine profile. Fold expression of mRNA for pro-inflammatory *Tnf* (A), *Il1b* (B), and *Il6* (C) and anti-inflammatory *Il10* (D) in hippocampus of vehicle- or BuNa-treated mice injected PTX (n = 6 per group). The effect of PTX on cytokine levels was compared to vehicle group. Results are shown as mean ± SEM. Differences were analyzed using ANOVA followed by Tukey's post hoc test for multiple comparisons. *p < 0.05, **p < 0.01, and ***p < 0.001 versus relative control.

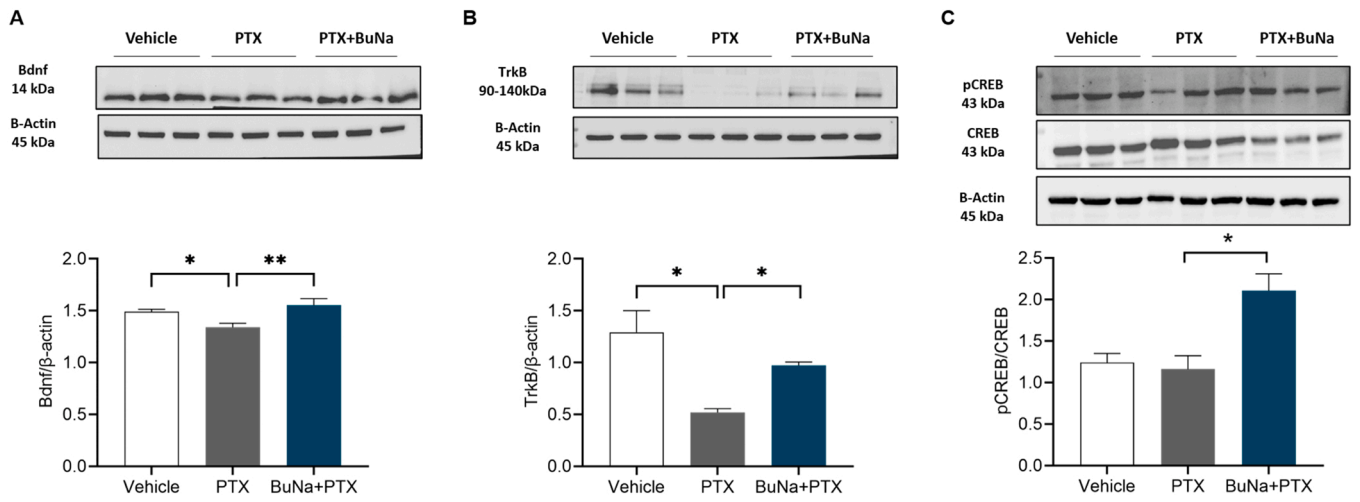

Fig. 8. Western blot analyses of BDNF (A), TrkB (B) and pCREB/CREB (C) in the hippocampus of PTX-treated mice. An image depicting three representative samples for each immunoblot is reported. In the densitometry analysis of n = 6 mice per group, results are shown as mean ± SEM. Differences were analyzed by ANOVA followed by Tukey's post hoc test for multiple comparisons, *p < 0.05, **p < 0.01 versus relative control.

characterized by altered levels of butyrate, which have been reported to induce not only intestinal manifestations, but also impaired cognitive function [73].

Compelling evidence has suggested the therapeutic use of butyrate in the improvement of inflammation, oxidative stress, mucosal defense mechanisms, and intestinal motility [52–54].

The SCFA, metabolites derived from the bacterial fermentation of dietary fibers, are fuels for intestinal epithelial cells, impact on gut motility and strengthen the gut barrier functions, all conditions crucial to maintain intestinal homeostasis. Recent findings show that among SCFA, butyrate shows different intestinal and immuno-modulatory functions and has been also proposed as compound able to modulate neurodevelopment and behavioral dysfunctions [57], without causing adverse effects. Indeed, in animal models, administration of butyrate has been shown to ameliorate vascular dementia [74,75] and cognitive impairment [76,77], as well as metabolic risk factors for cognitive decline and dementia [78].

In light of available literature and pharmacological and clinical data, BuNa is a safe supplement used for the treatment and the prevention of different conditions mostly affecting the digestive tract (i.e., diarrhea, dysbiosis, irritable bowel syndroms or inflammatory conditions), with minimal or absent side effects at the standard or higher dose. Specifically, in humans BuNa is used in a common rage dose from 150 to 300 mg/day [79]; however also higher dose (4 g of butyrate per day) showed beneficial effects in obese and healthy patients with an acceptable safety profile [80]. However, the limitation of BuNa in clinics is due to its negative organoleptic properties characterized by unpleasant taste and odor [81], requiring optimization of its formulations. On the contrary, different doses of BuNa are used in mice depending on the pathological conditions studied. In mice, the maximum tolerated dose of BuNa is 1.25 g/kg [82]. Thus, the dose used in the present study (30 mg/kg), equal to 3,3 mg/kg for humans, was well tolerated and safe in mice.

Similar to patients undergoing chemotherapy [37], one cycle of PTX, here resulted in reduced fecal levels of butyrate, suggesting the disruptive nature of this chemotherapeutics on gut microbiota.

The bidirectional communication between the intestine and the CNS is one of the most intriguing objects of investigation in the last decades, highlighting the imperative role the microbiota-gut-brain axis in the regulation of body homeostasis.

Although a definitive mechanism of gut-brain interaction has not been fully established, multiple pathways have been proposed, including direct neural communication and/or humoral communication through inflammatory mediators or bacterial products released into the bloodstream and reaching the central nervous system [83–85]. In this scenario, growing evidence show a role of microbiota-generated short-chain fatty acids [86,87], among which BuNa particularly influencing brain functions and behavior [78,88]. Several studies in different conditions reported that BuNa can enhance the proportion of cholinergic enteric neurons via epigenetic mechanisms [89] or send signals from the gut to brain through the cAMP signaling pathway [90,91]. On the other hand, BuNa can activate the vagus nerve and hypothalamus, crossing the BBB, and send efferent signals to the periphery [92,93]. Although in our model it is not intuitive a detailed BuNa-mediated mechanism of action at molecular level, based on our results we hypothesize that the restoration of eubiosis and the resolution of inflammation leads to BuNa's effect on central level.

The gastrointestinal tract is one of the major targets of chemotherapy toxicity impacting body weight, gut barrier integrity and motility as well as microbiota composition [33–37]. These alterations have proven to impinge brain functions and overall behavior [38–41]. Studies carried out in our laboratories have previously demonstrated that a probiotic formulation prevents CIPN and preserves gut integrity in a model of chemotherapy-induced neuropathy [72]. Here, we found that PTX treatment induced moderate sickness-like behavior in mice, as revealed by reduction of body weight, food intake, and latency to eat in the novelty suppressed feeding test. The weight loss and the reduced food intake are common side effects of paclitaxel [94] and other chemotherapies in cancer patients, that may lead to mortality [95,96]. In addition, PTX treatment also altered microbiota and gut permeability leading to systemic inflammation. Indeed, PTX perturbed microbiota structure and composition mainly influencing the balance between Bacteroidetes and Firmicutes. Specific species belonging to the Bacteroidetes phylum marked the microbiota of PTX group: increased *Odoribacter splanchnicus, Muribaculum intestinale,* and *Prevotella stercorea,* and reduced *Alistipes senegalensis*. Notably, BuNa administration restored altered Bacteroidetes/Firmicutes ratio mainly impacting on *O. splanchnicus* and *P. stercorea* levels. Genus *Prevotella* is able to promote intestinal dysbiosis and inflammation and to decrease the levels of SCFAs [97]. BuNa treatment prevents the loss of body weight and modulates microbiota composition affecting levels of bacterial genera involved in SCFAs production. Moreover, the reduction of the acetate-producer *Alistipes senegalensis* in mice treated with PTX was accompanied by a decrease of fecal acetate and butyrate levels. Upon BuNa administration a new metabolic network sustained by the acetate- and butyrate-producing *Clostridium saccharolitycum* is established. This

is accompanied by increased levels of acetate and butyrate in feces. We cannot exclude that the high levels of fecal butyrate derive from its exogenous administration, however, it is sustainable the hypothesis of BuNa effect through microbiota metabolism and gut-brain axis modulation. The preventive treatment with BuNa was also able to repristinate intestinal permeability and levels of tight junctions' protein in PTX-treated mice.

SCFAs are able to cross the BBB and influence brain processes, including cell proliferation, differentiation, and gene expression [98] in particular, butyrate which is an extremely important source of energy for colonocytes, shows also a plethora of effects on neuronal cells, by controlling myelination [99], amyloidgenesis [100], as well as promoting neuroprotection in models of neurodegenerative disease [101]. Indeed, in our experiments BuNa treatment counteracted the pro-inflammatory signature induced by PTX at both systemic and hippocampal levels. Moreover, the reduction of neuro-inflammation mediated by BuNa was associated with an improvement in behavioral changes confirming its antidepressant and anxiolytic action [55]. Mechanistically, BuNa treatment restored BDNF/TrkB signaling pathway in the hippocampal region downregulated by PTX, and in line within previous studies [102,103]. Growing evidence suggests that BDNF mitigates depressive symptoms binding TrkB, leading to the activation of downstream signaling molecules [104]. CREB is usually up-regulated by chronic antidepressant treatment, and the increased CREB levels in rodent model results in antidepressant-like behaviors [105]. In agreement with that, BuNa significantly increased the ratio of pCREB/CREB in PTX-treated mice. Altogether these data demonstrate a clear central effect of BuNa in preventing neuro-inflammation and perturbations in BDNF signaling pathway in PTX-treated mice.

5. Conclusions

Here we demonstrate that the prolonged administration and stimulation of BuNa production by bacterial communities in PXT treated mice, improves intestinal function resulting also in a reorganization of the bacterial species, which in turn may improve inflammation at the central level and eventually behavioral symptoms. Specifically, the present work shows that microbiota and gut barrier perturbations induced by PTX lead to a systemic inflammation and depressive- and anxiety- like behaviors associated with molecular and functional changes in the hippocampus. Remarkably, repeated intake of the BuNa improves both central and peripheral side effects associated with PTX. Overall, BuNa was able to counteract PTX-induced depressive- and anxiety- like behaviors, resulting in the reduction in immobility time, decreasing the inflammation and maintaining gut integrity. More studies are needed to explore the mechanism of action of BuNa in PTX-associated metabolic and behavioral impairments and, the correlation between gut and the brain. However, our results prompt us to hypothesize that BuNa's effect on central outcomes of PTX occurs through the restoration of eubiosis and the resolution of inflammation.

On this basis, it is possible to propose the use of sodium butyrate during chemotherapy cycles as a valid adjuvant to decrease central and gastrointestinal side effects of chemotherapy. However, although it is already used in humans without side effects, additional studies might be required to identify new formulations able to improve patient's compliance.

Funding

This research did not receive any specific grant from funding agencies in the public, commercial, or not-for-profit sectors.

CRediT authorship contribution statement

C.C., F.M.L. and R.R. conceived and performed the in vivo and behavioral experiments and analyzed the data. M.C., and C.A. performed western blot and GS-MS experiments and analyzed the data. F.C. and M.P.M. performed ELISA and RT-PCR experiments and analyzed the data. I.T., L.C. and F.L. performed the microbiota experiments and analyzed the data. C.C., and R.R. conceived, designed the study. C.C., and R.R. wrote and revised the manuscript. GA, M.C., L.C., F. L., and M.P.M. contributed to the discussion and to the editing of the manuscript. All authors have approved the final version of the manuscript.

Declaration of Competing Interest

None.

Acknowledgements

We thank Giovanni Esposito, and Angelo Russo for animal care and assistance.

References

[1] M.J. Massie, Prevalence of depression in patients with cancer, J. Natl. Cancer Inst. Monogr. 2004 (2004) 57–71, https://doi.org/10.1093/jncimonographs/lgh014.
[2] A. Mehnert, E. Brähler, H. Faller, M. Härter, M. Keller, H. Schulz, K. Wegscheider, J. Weis, A. Boehncke, B. Hund, K. Reuter, M. Richard, S. Sehner, S. Sommerfeldt, C. Szalai, H.-U. Wittchen, U. Koch, Four-week prevalence of mental disorders in patients with cancer across major tumor entities, JCO 32 (2014) 3540–3546, https://doi.org/10.1200/JCO.2014.56.0086.
[3] A.M.H. Krebber, L.M. Buffart, G. Kleijn, I.C. Riepma, R. Bree, C.R. Leemans, A. Becker, J. Brug, A. Straten, P. Cuijpers, I.M. Verdonck-de Leeuw, Prevalence of depression in cancer patients: a meta-analysis of diagnostic interviews and self-report instruments, Psycho-Oncology 23 (2014) 121–130, https://doi.org/10.1002/pon.3409.
[4] K.D. van der Willik, V. Koppelmans, M. Hauptmann, A. Compter, M.A. Ikram, S. B. Schagen, Inflammation markers and cognitive performance in breast cancer survivors 20 years after completion of chemotherapy: a cohort study, Breast Cancer Res. 20 (2018) 135, https://doi.org/10.1186/s13058-018-1062-3.
[5] S. Kesler, M. Janelsins, D. Koovakkattu, O. Palesh, K. Mustian, G. Morrow, F. S. Dhabhar, Reduced hippocampal volume and verbal memory performance associated with interleukin-6 and tumor necrosis factor-alpha levels in chemotherapy-treated breast cancer survivors, Brain Behav. Immun. 30 (2013) S109–S116, https://doi.org/10.1016/j.bbi.2012.05.017.
[6] V. Koppelmans, M.M.B. Breteler, W. Boogerd, C. Seynaeve, C. Gundy, S. B. Schagen, Neuropsychological performance in survivors of breast cancer more than 20 years after adjuvant chemotherapy, JCO 30 (2012) 1080–1086, https://doi.org/10.1200/JCO.2011.37.0189.
[7] J.J. Olin, Cognitive function after systemic therapy for breast cancer, Oncology 15 (2001) 613–618, discussion 618, 621–624.
[8] J.L. Vardy, H.M. Dhillon, G.R. Pond, S.B. Rourke, T. Bekele, C. Renton, A. Dodd, H. Zhang, P. Beale, S. Clarke, I.F. Tannock, Cognitive function in patients with colorectal cancer who do and do not receive chemotherapy: a prospective, longitudinal, controlled study, JCO 33 (2015) 4085–4092, https://doi.org/10.1200/JCO.2015.63.0905.
[9] N. Cerulla Torrente, J.-B. Navarro Pastor, N. de la Osa Chaparro, Systematic review of cognitive sequelae of non-central nervous system cancer and cancer therapy, J. Cancer Surviv. 14 (2020) 464–482, https://doi.org/10.1007/s11764-020-00870-2.
[10] Y.T. Cheung, T. Ng, M. Shwe, H.K. Ho, K.M. Foo, M.T. Cham, J.A. Lee, G. Fan, Y. P. Tan, W.S. Yong, P. Madhukumar, S.K. Loo, S.F. Ang, M. Wong, W.Y. Chay, W. S. Ooi, R.A. Dent, Y.S. Yap, R. Ng, A. Chan, Association of proinflammatory cytokines and chemotherapy-associated cognitive impairment in breast cancer patients: a multi-centered, prospective, cohort study, Ann. Oncol. 26 (2015) 1446–1451, https://doi.org/10.1093/annonc/mdv206.
[11] M. Markman, T.M. Mekhail, Paclitaxel in cancer therapy, Expert Opin. Pharmacother. 3 (2002) 755–766, https://doi.org/10.1517/14656566.3.6.755.
[12] G. Alloatti, C. Penna, M.P. Gallo, R.C. Levi, E. Bombardelli, G. Appendino, Differential effects of paclitaxel and derivatives on guinea pig isolated heart and papillary muscle, J. Pharm. Exp. Ther. 284 (1998) 561–567.
[13] C.G. Ziske, B. Schöttker, M. Gorschlüter, U. Mey, R. Kleinschmidt, U. Schlegel, T. Sauerbruch, I.G.H. Schmidt-Wolf, Acute transient encephalopathy after paclitaxel infusion: report of three cases, Ann. Oncol. 13 (2002) 629–631, https://doi.org/10.1093/annonc/mdf025.
[14] R. Walz, M.M. Bianchin, F. Kliemann, Transient encephalopathy after Taxol infusion, Neurology 49 (1997) 1188.2–1189, https://doi.org/10.1212/WNL.49.4.1188-a.
[15] Y. Nieto, P.J. Cagnoni, S.I. Bearman, E.J. Shpall, S. Matthes, T. DeBoom, A. Barón, R.B. Jones, Acute encephalopathy: a new toxicity associated with high-dose paclitaxel, Clin. Cancer Res. 5 (1999) 501–506.
[16] S. Muallaoğlu, M. Koçer, N. Güler, Acute transient encephalopathy after weekly paclitaxel infusion, Med. Oncol. 29 (2012) 1297–1299, https://doi.org/10.1007/s12032-011-9956-2.

[17] P. Huehnchen, W. Boehmerle, A. Springer, D. Freyer, M. Endres, A novel preventive therapy for paclitaxel-induced cognitive deficits: preclinical evidence from C57BL/6 mice, Transl. Psychiatry 7 (2017), https://doi.org/10.1038/tp.2017.149 (e1185–e1185).

[18] L.T. Young, Neuroprotective effects of antidepressant and mood stabilizing drugs, J. Psychiatry Neurosci. 27 (2002) 8–9.

[19] W. Deng, J.B. Aimone, F.H. Gage, New neurons and new memories: how does adult hippocampal neurogenesis affect learning and memory? Nat. Rev. Neurosci. 11 (2010) 339–350, https://doi.org/10.1038/nrn2822.

[20] H. Wang, J. Warner-Schmidt, S. Varela, G. Enikolopov, P. Greengard, M. Flajolet, Norbin ablation results in defective adult hippocampal neurogenesis and depressive-like behavior in mice, Proc. Natl. Acad. Sci. USA 112 (2015) 9745–9750, https://doi.org/10.1073/pnas.1510291112.

[21] N. Rocamora, F.J. García-Ladona, J.M. Palacios, G. Mengod, Differential expression of brain-derived neurotrophic factor, neurotrophin-3, and low-affinity nerve growth factor receptor during the postnatal development of the rat cerebellar system, Mol. Brain Res. 17 (1993) 1–8, https://doi.org/10.1016/0169-328X(93)90065-W.

[22] R.H. Lipsky, A.M. Marini, Brain-derived neurotrophic factor in neuronal survival and behavior-related plasticity, Ann. N. Y. Acad. Sci. 1122 (2007) 130–143, https://doi.org/10.1196/annals.1403.009.

[23] L. Novikova, L. Novikov, J.-O. Kellerth, Brain-derived neurotrophic factor reduces necrotic zone and supports neuronal survival after spinal cord hemisection in adult rats, Neurosci. Lett. 220 (1996) 203–206, https://doi.org/10.1016/S0304-3940(96)13267-5.

[24] D. Azoulay, A. Leibovici, R. Sharoni, E. Shaoul, B. Gross, A. Braester, H. Goldberg, Association between Met-BDNF allele and vulnerability to paclitaxel-induced peripheral neuropathy, Breast Cancer Res. Treat. 153 (2015) 703–704, https://doi.org/10.1007/s10549-015-3546-5.

[25] C. Scripture, W. Figg, A. Sparreboom, Peripheral neuropathy induced by paclitaxel: recent insights and future perspectives, CN 4 (2006) 165–172, https://doi.org/10.2174/157015906776359568.

[26] N. Tsavaris, C. Kosmas, M. Vadiaka, P. Kanelopoulos, D. Boulamatsis, Immune changes in patients with advanced breast cancer undergoing chemotherapy with taxanes, Br. J. Cancer 87 (2002) 21–27, https://doi.org/10.1038/sj.bjc.6600347.

[27] L. Pusztai, T.R. Mendoza, J.M. Reuben, M.M. Martinez, J.S. Willey, J. Lara, A. Syed, H.A. Fritsche, E. Bruera, D. Booser, V. Valero, B. Arun, N. Ibrahim, E. Rivera, M. Royce, C.S. Cleeland, G.N. Hortobagyi, Changes in plasma levels of inflammatory cytokines in response to paclitaxel chemotherapy, Cytokine 25 (2004) 94–102, https://doi.org/10.1016/j.cyto.2003.10.004.

[28] X.-M. Wang, B. Walitt, L. Saligan, A.F. Tiwari, C.W. Cheung, Z.-J. Zhang, Chemobrain: a critical review and causal hypothesis of link between cytokines and epigenetic reprogramming associated with chemotherapy, Cytokine 72 (2015) 86–96, https://doi.org/10.1016/j.cyto.2014.12.006.

[29] Z. Li, S. Zhao, H.-L. Zhang, P. Liu, F.-F. Liu, Y.-X. Guo, X.-L. Wang, Proinflammatory factors mediate paclitaxel-induced impairment of learning and memory, Mediat. Inflamm. 2018 (2018) 1–9, https://doi.org/10.1155/2018/3941840.

[30] C.A. Murray, M.A. Lynch, Evidence that increased hippocampal expression of the cytokine interleukin-1β is a common trigger for age- and stress-induced impairments in long-term potentiation, J. Neurosci. 18 (1998) 2974–2981, https://doi.org/10.1523/JNEUROSCI.18-08-02974.1998.

[31] V. Tancredi, M. D'Antuono, C. Cafè, S. Giovedì, M.C. Buè, G. D'Arcangelo, F. Onofri, F. Benfenati, The inhibitory effects of interleukin-6 on synaptic plasticity in the rat hippocampus are associated with an inhibition of mitogen-activated protein kinase ERK, J. Neurochem. 75 (2002) 634–643, https://doi.org/10.1046/j.1471-4159.2000.0750634.x.

[32] R. Costa, G.F. Passos, N.L.M. Quintão, E.S. Fernandes, J.R.L.C.B. Maia, M. M. Campos, J.B. Calixto, Taxane-induced neurotoxicity: pathophysiology and therapeutic perspectives, Br. J. Pharm. 177 (2020) 3127–3146, https://doi.org/10.1111/bph.15086.

[33] E. Montassier, E. Batard, S. Massart, T. Gastinne, T. Carton, J. Caillon, S. Le Fresne, N. Caroff, J.B. Hardouin, P. Moreau, G. Potel, F. Le Vacon, M.F. de La Cochetière, 16S rRNA gene pyrosequencing reveals shift in patient faecal microbiota during high-dose chemotherapy as conditioning regimen for bone marrow transplantation, Microb. Ecol. 67 (2014) 690–699, https://doi.org/10.1007/s00248-013-0355-4.

[34] A.M. Stringer, N. Al-Dasooqi, J.M. Bowen, T.H. Tan, M. Radzuan, R.M. Logan, B. Mayo, D.M.K. Keefe, R.J. Gibson, Biomarkers of chemotherapy-induced diarrhoea: a clinical study of intestinal microbiome alterations, inflammation and circulating matrix metalloproteinases, Support Care Cancer 21 (2013) 1843–1852, https://doi.org/10.1007/s00520-013-1741-7.

[35] M.J. van Vliet, W.J.E. Tissing, C.A.J. Dun, N.E.L. Meessen, W.A. Kamps, E.S.J. M. de Bont, H.J.M. Harmsen, Chemotherapy treatment in pediatric patients with acute myeloid leukemia receiving antimicrobial prophylaxis leads to a relative increase of colonization with potentially pathogenic bacteria in the gut, Clin. Infect. Dis. 49 (2009) 262–270, https://doi.org/10.1086/599346.

[36] J. Zwielehner, C. Lassl, B. Hippe, A. Pointner, O.J. Switzeny, M. Remely, E. Kitzweger, R. Ruckser, A.G. Haslberger, Changes in human fecal microbiota due to chemotherapy analyzed by TaqMan-PCR, 454 sequencing and PCR-DGGE fingerprinting, PLoS One 6 (2011), e28654, https://doi.org/10.1371/journal.pone.0028654.

[37] E. Montassier, T. Gastinne, P. Vangay, G.A. Al-Ghalith, S. Bruley des Varannes, S. Massart, P. Moreau, G. Potel, M.F. de La Cochetière, E. Batard, D. Knights, Chemotherapy-driven dysbiosis in the intestinal microbiome, Aliment. Pharm. Ther. 42 (2015) 515–528, https://doi.org/10.1111/apt.13302.

[38] B. Gustorff, T. Dorner, R. Likar, W. Grisold, K. Lawrence, F. Schwarz, A. Rieder, Prevalence of self-reported neuropathic pain and impact on quality of life: a prospective representative survey: neuropathic pain in Austria, Acta Anaesthesiol. Scand. 52 (2007) 132–136, https://doi.org/10.1111/j.1399-6576.2007.01486.x.

[39] P. Bercik, E. Denou, J. Collins, W. Jackson, J. Lu, J. Jury, Y. Deng, P. Blennerhassett, J. Macri, K.D. McCoy, E.F. Verdu, S.M. Collins, The intestinal microbiota affect central levels of brain-derived neurotropic factor and behavior in mice, Gastroenterology 141 (2011) 599–609.e3, https://doi.org/10.1053/j.gastro.2011.04.052.

[40] L. Desbonnet, G. Clarke, A. Traplin, O. O'Sullivan, F. Crispie, R.D. Moloney, P. D. Cotter, T.G. Dinan, J.F. Cryan, Gut microbiota depletion from early adolescence in mice: implications for brain and behaviour, Brain Behav., Immun. 48 (2015) 165–173, https://doi.org/10.1016/j.bbi.2015.04.004.

[41] E.E. Fröhlich, A. Farzi, R. Mayerhofer, F. Reichmann, A. Jačan, B. Wagner, E. Zinser, N. Bordag, C. Magnes, E. Fröhlich, K. Kashofer, G. Gorkiewicz, P. Holzer, Cognitive impairment by antibiotic-induced gut dysbiosis: analysis of gut microbiota-brain communication, Brain Behav. Immun. 56 (2016) 140–155, https://doi.org/10.1016/j.bbi.2016.02.020.

[42] C.V. Grant, B.R. Loman, M.T. Bailey, L.M. Pyter, Manipulations of the gut microbiome alter chemotherapy-induced inflammation and behavioral side effects in female mice, Brain Behav. Immun. 95 (2021) 401–412, https://doi.org/10.1016/j.bbi.2021.04.014.

[43] Q. Le Bastard, T. Ward, D. Sidiropoulos, B.M. Hillmann, C.L. Chun, M. J. Sadowsky, D. Knights, E. Montassier, Fecal microbiota transplantation reverses antibiotic and chemotherapy-induced gut dysbiosis in mice, Sci. Rep. 8 (2018) 6219, https://doi.org/10.1038/s41598-018-24342-x.

[44] Y. Wu, J. Wu, Z. Lin, Q. Wang, Y. Li, A. Wang, X. Shan, J. Liu, Administration of a probiotic mixture ameliorates cisplatin-induced mucositis and pica by regulating 5-HT in rats, J. Immunol. Res. 2021 (2021) 1–16, https://doi.org/10.1155/2021/9321196.

[45] A.M. Stringer, R.J. Gibson, J.M. Bowen, R.M. Logan, K. Ashton, A.S.J. Yeoh, N. Al-Dasooqi, D.M.K. Keefe, Irinotecan-induced mucositis manifesting as diarrhoea corresponds with an amended intestinal flora and mucin profile, Int. J. Exp. Pathol. 90 (2009) 489–499, https://doi.org/10.1111/j.1365-2613.2009.00671.x.

[46] I. von Bültzingslöwen, I. Adlerberth, A.E. Wold, G. Dahlén, M. Jontell, Oral and intestinal microflora in 5-fluorouracil treated rats, translocation to cervical and mesenteric lymph nodes and effects of probiotic bacteria: 5-FU and microflora, translocation and effects of probiotics, Oral Microbiol. Immunol. 18 (2003) 278–284, https://doi.org/10.1034/j.1399-302X.2003.00075.x.

[47] B.R. Loman, K.R. Jordan, B. Haynes, M.T. Bailey, L.M. Pyter, Chemotherapy-induced neuroinflammation is associated with disrupted colonic and bacterial homeostasis in female mice, Sci. Rep. 9 (2019) 16490, https://doi.org/10.1038/s41598-019-52893-0.

[48] J.H. Cummings, E.W. Pomare, W.J. Branch, C.P. Naylor, G.T. Macfarlane, Short chain fatty acids in human large intestine, portal, hepatic and venous blood, Gut 28 (1987) 1221–1227, https://doi.org/10.1136/gut.28.10.1221.

[49] A. Wang, Z. Ling, Z. Yang, P.R. Kiela, T. Wang, C. Wang, L. Cao, F. Geng, M. Shen, X. Ran, Y. Su, T. Cheng, J. Wang, Gut microbial dysbiosis may predict diarrhea and fatigue in patients undergoing pelvic cancer radiotherapy: a pilot study, PLoS One 10 (2015), e0126312, https://doi.org/10.1371/journal.pone.0126312.

[50] T. Tian, Y. Zhao, Y. Yang, T. Wang, S. Jin, J. Guo, Z. Liu, The protective role of short-chain fatty acids acting as signal molecules in chemotherapy- or radiation-induced intestinal inflammation, Am. J. Cancer Res. 10 (2020) 3508–3531.

[51] R.B. Canani, M. Di Costanzo, L. Leone, G. Bedogni, P. Brambilla, S. Cianfarani, V. Nobili, A. Pietrobelli, C. Agostoni, Epigenetic mechanisms elicited by nutrition in early life, Nutr. Res. Rev. 24 (2011) 198–205, https://doi.org/10.1017/S0954422411000102.

[52] J.-P. Segain, Butyrate inhibits inflammatory responses through NFkappa B inhibition: implications for Crohn's disease, Gut 47 (2000) 397–403, https://doi.org/10.1136/gut.47.3.397.

[53] E.L.M. Vieira, A.J. Leonel, A.P. Sad, N.R.M. Beltrão, T.F. Costa, T.M.R. Ferreira, A. C. Gomes-Santos, A.M.C. Faria, M.C.G. Peluzio, D.C. Cara, J.I. Alvarez-Leite, Oral administration of sodium butyrate attenuates inflammation and mucosal lesion in experimental acute ulcerative colitis, J. Nutr. Biochem. 23 (2012) 430–436, https://doi.org/10.1016/j.jnutbio.2011.01.007.

[54] H.M. Hamer, D.M.A.E. Jonkers, A. Bast, S.A.L.W. Vanhoutvin, M.A.J.G. Fischer, A. Kodde, F.J. Troost, K. Venema, R.-J.M. Brummer, Butyrate modulates oxidative stress in the colonic mucosa of healthy humans, Clin. Nutr. 28 (2009) 88–93, https://doi.org/10.1016/j.clnu.2008.11.002.

[55] L. Zheng, C.J. Kelly, K.D. Battista, R. Schaefer, J.M. Lanis, E.E. Alexeev, R. X. Wang, J.C. Onyiah, D.J. Kominsky, S.P. Colgan, Microbial-derived butyrate promotes epithelial barrier function through IL-10 receptor–dependent repression of claudin-2, J. Immunol. 199 (2017) 2976–2984, https://doi.org/10.4049/jimmunol.1700105.

[56] F.A. Schroeder, C.L. Lin, W.E. Crusio, S. Akbarian, Antidepressant-like effects of the histone deacetylase inhibitor, sodium butyrate, in the mouse, Biol. Psychiatry 62 (2007) 55–64, https://doi.org/10.1016/j.biopsych.2006.06.036.

[57] W. Toma, S.L. Kyte, D. Bagdas, Y. Alkhlaif, S.D. Alsharari, A.H. Lichtman, Z.-J. Chen, E. Del Fabbro, J.W. Bigbee, D.A. Gewirtz, M.I. Damaj, Effects of paclitaxel on the development of neuropathy and affective behaviors in the mouse, Neuropharmacology 117 (2017) 305–315, https://doi.org/10.1016/j.neuropharm.2017.02.020.

[58] J. Liu, F. Wang, S. Liu, J. Du, X. Hu, J. Xiong, R. Fang, W. Chen, J. Sun, Sodium butyrate exerts protective effect against Parkinson's disease in mice via

stimulation of glucagon like peptide-1, J. Neurol. Sci. 381 (2017) 176–181, https://doi.org/10.1016/j.jns.2017.08.3235.
[59] C.B. de La Serre, C.L. Ellis, J. Lee, A.L. Hartman, J.C. Rutledge, H.E. Raybould, Propensity to high-fat diet-induced obesity in rats is associated with changes in the gut microbiota and gut inflammation, Am. J. Physiol.-Gastrointest. Liver Physiol. 299 (2010) G440–G448, https://doi.org/10.1152/ajpgi.00098.2010.
[60] L. Coretti, C. Cristiano, E. Florio, G. Scala, A. Lama, S. Keller, M. Cuomo, R. Russo, R. Pero, O. Paciello, G. Mattace Raso, R. Meli, S. Cocozza, A. Calignano, L. Chiariotti, F. Lembo, Sex-related alterations of gut microbiota composition in the BTBR mouse model of autism spectrum disorder, Sci. Rep. 7 (2017) 45356, https://doi.org/10.1038/srep45356.
[61] E. Bolyen, J.R. Rideout, M.R. Dillon, N.A. Bokulich, C.C. Abnet, G.A. Al-Ghalith, H. Alexander, E.J. Alm, M. Arumugam, F. Asnicar, Y. Bai, J.E. Bisanz, K. Bittinger, A. Brejnrod, C.J. Brislawn, C.T. Brown, B.J. Callahan, A.M. Caraballo-Rodríguez, J. Chase, E.K. Cope, R. Da Silva, C. Diener, P.C. Dorrestein, G.M. Douglas, D. M. Durall, C. Duvallet, C.F. Edwardson, M. Ernst, M. Estaki, J. Fouquier, J. M. Gauglitz, S.M. Gibbons, D.L. Gibson, A. Gonzalez, K. Gorlick, J. Guo, B. Hillmann, S. Holmes, H. Holste, C. Huttenhower, G.A. Huttley, S. Janssen, A. K. Jarmusch, L. Jiang, B.D. Kaehler, K.B. Kang, C.R. Keefe, P. Keim, S.T. Kelley, D. Knights, I. Koester, T. Kosciolek, J. Kreps, M.G.I. Langille, J. Lee, R. Ley, Y.-X. Liu, E. Loftfield, C. Lozupone, M. Maher, C. Marotz, B.D. Martin, D. McDonald, L.J. McIver, A.V. Melnik, J.L. Metcalf, S.C. Morgan, J.T. Morton, A.T. Naimey, J. A. Navas-Molina, L.F. Nothias, S.B. Orchanian, T. Pearson, S.L. Peoples, D. Petras, M.L. Preuss, E. Pruesse, L.B. Rasmussen, A. Rivers, M.S. Robeson, P. Rosenthal, N. Segata, M. Shaffer, A. Shiffer, R. Sinha, S.J. Song, J.R. Spear, A.D. Swafford, L. R. Thompson, P.J. Torres, P. Trinh, A. Tripathi, P.J. Turnbaugh, S. Ul-Hasan, J.J. J. van der Hooft, F. Vargas, Y. Vázquez-Baeza, E. Vogtmann, M. von Hippel, W. Walters, Y. Wan, M. Wang, J. Warren, K.C. Weber, C.H.D. Williamson, A. D. Willis, Z.Z. Xu, J.R. Zaneveld, Y. Zhang, Q. Zhu, R. Knight, J.G. Caporaso, Reproducible, interactive, scalable and extensible microbiome data science using QIIME 2, Nat. Biotechnol. 37 (2019) 852–857, https://doi.org/10.1038/s41587-019-0209-9.
[62] B.J. Callahan, P.J. McMurdie, M.J. Rosen, A.W. Han, A.J.A. Johnson, S.P. Holmes, DADA2: high-resolution sample inference from Illumina amplicon data, Nat. Methods 13 (2016) 581–583, https://doi.org/10.1038/nmeth.3869.
[63] B.D. Kaehler, N.A. Bokulich, D. McDonald, R. Knight, J.G. Caporaso, G.A. Huttley, Species abundance information improves sequence taxonomy classification accuracy, Nat. Commun. 10 (2019) 4643, https://doi.org/10.1038/s41467-019-12669-6.
[64] N.A. Bokulich, B.D. Kaehler, J.R. Rideout, M. Dillon, E. Bolyen, R. Knight, G. A. Huttley, J. Gregory Caporaso, Optimizing taxonomic classification of marker-gene amplicon sequences with QIIME 2's q2-feature-classifier plugin, Microbiome 6 (2018) 90, https://doi.org/10.1186/s40168-018-0470-z.
[65] D. McDonald, M.N. Price, J. Goodrich, E.P. Nawrocki, T.Z. DeSantis, A. Probst, G. L. Andersen, R. Knight, P. Hugenholtz, An improved Greengenes taxonomy with explicit ranks for ecological and evolutionary analyses of bacteria and archaea, ISME J. 6 (2012) 610–618, https://doi.org/10.1038/ismej.2011.139.
[66] C. Camacho, G. Coulouris, V. Avagyan, N. Ma, J. Papadopoulos, K. Bealer, T. L. Madden, BLAST+: architecture and applications, BMC Bioinform. 10 (2009) 421, https://doi.org/10.1186/1471-2105-10-421.
[67] N. Segata, J. Izard, L. Waldron, D. Gevers, L. Miropolsky, W.S. Garrett, C. Huttenhower, Metagenomic biomarker discovery and explanation, Genome Biol. 12 (2011) R60, https://doi.org/10.1186/gb-2011-12-6-r60.
[68] J.D. Hunter, Matplotlib: a 2D graphics environment, Comput. Sci. Eng. 9 (2007) 90–95, https://doi.org/10.1109/MCSE.2007.55.
[69] M.J. Curtis, S. Alexander, G. Cirino, J.R. Docherty, C.H. George, M.A. Giembycz, D. Hoyer, P.A. Insel, A.A. Izzo, Y. Ji, D.J. MacEwan, C.G. Sobey, S.C. Stanford, M. M. Teixeira, S. Wonnacott, A. Ahluwalia, Experimental design and analysis and their reporting II: updated and simplified guidance for authors and peer reviewers: editorial, Br. J. Pharm. 175 (2018) 987–993, https://doi.org/10.1111/bph.14153.
[70] C. Martin-Gallausiaux, L. Marinelli, H.M. Blottière, P. Larraufie, N. Lapaque, SCFA: mechanisms and functional importance in the gut, Proc. Nutr. Soc. 80 (2021) 37–49, https://doi.org/10.1017/S0029665120006916.
[71] Y.F. Li, C. Zhang, S. Zhou, M. He, H. Zhang, N. Chen, F. Li, X. Luan, M. Pai, H. Yuan, D. Sun, Y. Li, Species difference in paclitaxel disposition correlated with poor pharmacological efficacy translation from mice to humans, CPAA 10 (2018) 165–174, https://doi.org/10.2147/CPAA.S185449.
[72] M. Cuozzo, V. Castelli, C. Avagliano, A. Cimini, M. d'Angelo, C. Cristiano, R. Russo, Effects of chronic oral probiotic treatment in paclitaxel-induced neuropathic pain, Biomedicines 9 (2021) 346, https://doi.org/10.3390/biomedicines9040346.
[73] K. Meyer, A. Lulla, K. Debroy, J.M. Shikany, K. Yaffe, O. Meirelles, L.J. Launer, Association of the gut microbiota with cognitive function in midlife, JAMA Netw. Open 5 (2022), e2143941, https://doi.org/10.1001/jamanetworkopen.2021.43941.
[74] J. Liu, J. Sun, F. Wang, X. Yu, Z. Ling, H. Li, H. Zhang, J. Jin, W. Chen, M. Pang, J. Yu, Y. He, J. Xu, Neuroprotective effects of *Clostridium butyricum* against vascular dementia in mice via metabolic butyrate, BioMed Res. Int. 2015 (2015) 1–12, https://doi.org/10.1155/2015/412946.
[75] B. Sharma, N. Singh, Attenuation of vascular dementia by sodium butyrate in streptozotocin diabetic rats, Psychopharmacology 215 (2011) 677–687, https://doi.org/10.1007/s00213-011-2164-0.
[76] N. Govindarajan, R.C. Agis-Balboa, J. Walter, F. Sananbenesi, A. Fischer, Sodium butyrate improves memory function in an Alzheimer's disease mouse model when administered at an advanced stage of disease progression, JAD 26 (2011) 187–197, https://doi.org/10.3233/JAD-2011-110080.
[77] H. Liu, J.-J. Zhang, X. Li, Y. Yang, X.-F. Xie, K. Hu, Post-occlusion administration of sodium butyrate attenuates cognitive impairment in a rat model of chronic cerebral hypoperfusion, Pharm. Biochem. Behav. 135 (2015) 53–59, https://doi.org/10.1016/j.pbb.2015.05.012.
[78] I.A.C. Arnoldussen, M. Wiesmann, C.E. Pelgrim, E.M. Wielemaker, W. van Duyvenvoorde, P.L. Amaral-Santos, L. Verschuren, B.J.F. Keijser, A. Heerschap, R. Kleemann, P.Y. Wielinga, A.J. Kiliaan, Butyrate restores HFD-induced adaptations in brain function and metabolism in mid-adult obese mice, Int. J. Obes. 41 (2017) 935–944, https://doi.org/10.1038/ijo.2017.52.
[79] T. Banasiewicz, D. Domagalska, K. Borycka-Kiciak, G. Rydzewska, Determination of butyric acid dosage based on clinical and experimental studies – a literature review, Prz. Gastroenterol. 15 (2020) 119–125, https://doi.org/10.5114/pg.2020.95556.
[80] M.C.P. Cleophas, J.M. Ratter, S. Bekkering, J. Quintin, K. Schraa, E.S. Stroes, M. G. Netea, L.A.B. Joosten, Effects of oral butyrate supplementation on inflammatory potential of circulating peripheral blood mononuclear cells in healthy and obese males, Sci. Rep. 9 (2019) 775, https://doi.org/10.1038/s41598-018-37246-7.
[81] R. Russo, C. Santarcangelo, N. Badolati, E. Sommella, A. De Filippis, M. Dacrema, P. Campiglia, M. Stornaiuolo, M. Daglia, In vivo bioavailability and in vitro toxicological evaluation of the new butyric acid releaser N-(1-carbamoyl-2-phenyl-ethyl) butyramide, Biomed. Pharmacother. 137 (2021), 111385, https://doi.org/10.1016/j.biopha.2021.111385.
[82] M.J. Egorin, Z.-M. Yuan, D.L. Sentz, K. Plaisance, J.L. Eiseman, Plasma pharmacokinetics of butyrate after intravenous administration of sodium butyrate or oral administration of tributyrin or sodium butyrate to mice and rats, Cancer Chemother. Pharm. 43 (1999) 445–453, https://doi.org/10.1007/s002800050922.
[83] J.E. Bajic, I.N. Johnston, G.S. Howarth, M.R. Hutchinson, From the bottom-up: chemotherapy and gut-brain axis dysregulation, Front. Behav. Neurosci. 12 (2018) 104, https://doi.org/10.3389/fnbeh.2018.00104.
[84] S.M. Collins, M. Surette, P. Bercik, The interplay between the intestinal microbiota and the brain, Nat. Rev. Microbiol. 10 (2012) 735–742, https://doi.org/10.1038/nrmicro2876.
[85] J.F. Cryan, K.J. O'Riordan, C.S.M. Cowan, K.V. Sandhu, T.F.S. Bastiaanssen, M. Boehme, M.G. Codagnone, S. Cussotto, C. Fulling, A.V. Golubeva, K. E. Guzzetta, M. Jaggar, C.M. Long-Smith, J.M. Lyte, J.A. Martin, A. Molinero-Perez, G. Moloney, E. Morelli, E. Morillas, R. O'Connor, J.S. Cruz-Pereira, V. L. Peterson, K. Rea, N.L. Ritz, E. Sherwin, S. Spichak, E.M. Teichman, M. van de Wouw, A.P. Ventura-Silva, S.E. Wallace-Fitzsimons, N. Hyland, G. Clarke, T. G. Dinan, The microbiota-gut-brain axis, Physiol. Rev. 99 (2019) 1877–2013, https://doi.org/10.1152/physrev.00018.2018.
[86] B. Dalile, L. Van Oudenhove, B. Vervliet, K. Verbeke, The role of short-chain fatty acids in microbiota–gut–brain communication, Nat. Rev. Gastroenterol. Hepatol. 16 (2019) 461–478, https://doi.org/10.1038/s41575-019-0157-3.
[87] J. Lee, V.R. Venna, D.J. Durgan, H. Shi, J. Hudobenko, N. Putluri, J. Petrosino, L. D. McCullough, R.M. Bryan, Young versus aged microbiota transplants to germ-free mice: increased short-chain fatty acids and improved cognitive performance, Gut Microbes 12 (2020) 1814107, https://doi.org/10.1080/19490976.2020.1814107.
[88] R.M. Stilling, M. van de Wouw, G. Clarke, C. Stanton, T.G. Dinan, J.F. Cryan, The neuropharmacology of butyrate: the bread and butter of the microbiota-gut-brain axis, Neurochem. Int. 99 (2016) 110–132, https://doi.org/10.1016/j.neuint.2016.06.011.
[89] R. Soret, J. Chevalier, P. De Coppet, G. Poupeau, P. Derkinderen, J.P. Segain, M. Neunlist, Short-chain fatty acids regulate the enteric neurons and control gastrointestinal motility in rats, Gastroenterology 138 (2010) 1772–1782.e4, https://doi.org/10.1053/j.gastro.2010.01.053.
[90] R.M. Stilling, T.G. Dinan, J.F. Cryan, Microbial genes, brain & behaviour – epigenetic regulation of the gut-brain axis, Genes Brain Behav. 13 (2014) 69–86, https://doi.org/10.1111/gbb.12109.
[91] M.J. Keenan, J. Zhou, M. Hegsted, C. Pelkman, H.A. Durham, D.B. Coulon, R. J. Martin, Role of resistant starch in improving gut health, adiposity, and insulin resistance, Adv. Nutr. 6 (2015) 198–205, https://doi.org/10.3945/an.114.007419.
[92] M. van de Wouw, H. Schellekens, T.G. Dinan, J.F. Cryan, Microbiota-gut-brain axis: modulator of host metabolism and appetite, J. Nutr. 147 (2017) 727–745, https://doi.org/10.3945/jn.116.240481.
[93] H. Gagliano, R. Delgado-Morales, A. Sanz-Garcia, A. Armario, High doses of the histone deacetylase inhibitor sodium butyrate trigger a stress-like response, Neuropharmacology 79 (2014) 75–82, https://doi.org/10.1016/j.neuropharm.2013.10.031.
[94] M.A. Ray, R.A. Trammell, S. Verhulst, S. Ran, L.A. Toth, Development of a mouse model for assessing fatigue during chemotherapy, Comp. Med. 61 (2011) 119–130.
[95] B.J. O'Brien, J. Rusthoven, A. Rocchi, J. Latreille, S. Fine, T. Vandenberg, F. Laberge, Impact of chemotherapy-associated nausea and vomiting on patients' functional status and on costs: survey of five Canadian centres, CMAJ 149 (1993) 296–302.
[96] D. Osoba, B. Zee, D. Warr, J. Latreille, L. Kaizer, J. Pater, Effect of postchemotherapy nausea and vomiting on health-related quality of life, Support. Care Cancer 5 (1997) 307–313, https://doi.org/10.1007/s005200050078.
[97] A. Iljazovic, U. Roy, E.J.C. Gálvez, T.R. Lesker, B. Zhao, A. Gronow, L. Amend, S. E. Will, J.D. Hofmann, M.C. Pils, K. Schmidt-Hohagen, M. Neumann-Schaal,

T. Strowig, Perturbation of the gut microbiome by Prevotella spp. enhances host susceptibility to mucosal inflammation, Mucosal Immunol. 14 (2021) 113–124, https://doi.org/10.1038/s41385-020-0296-4.

[98] G. Frost, M.L. Sleeth, M. Sahuri-Arisoylu, B. Lizarbe, S. Cerdan, L. Brody, J. Anastasovska, S. Ghourab, M. Hankir, S. Zhang, D. Carling, J.R. Swann, G. Gibson, A. Viardot, D. Morrison, E. Louise Thomas, J.D. Bell, The short-chain fatty acid acetate reduces appetite via a central homeostatic mechanism, Nat. Commun. 5 (2014) 3611, https://doi.org/10.1038/ncomms4611.

[99] T. Chen, D. Noto, Y. Hoshino, M. Mizuno, S. Miyake, Butyrate suppresses demyelination and enhances remyelination, J. Neuroinflamm. 16 (2019) 165, https://doi.org/10.1186/s12974-019-1552-y.

[100] S.Y. Kim, C.W. Chae, H.J. Lee, Y.H. Jung, G.E. Choi, J.S. Kim, J.R. Lim, J.E. Lee, J. H. Cho, H. Park, C. Park, H.J. Han, Sodium butyrate inhibits high cholesterol-induced neuronal amyloidogenesis by modulating NRF2 stabilization-mediated ROS levels: involvement of NOX2 and SOD1, Cell Death Dis. 11 (2020) 469, https://doi.org/10.1038/s41419-020-2663-1.

[101] Y. Jiang, K. Li, X. Li, L. Xu, Z. Yang, Sodium butyrate ameliorates the impairment of synaptic plasticity by inhibiting the neuroinflammation in 5XFAD mice, Chem.-Biol. Interact. 341 (2021), 109452, https://doi.org/10.1016/j.cbi.2021.109452.

[102] P.-S. Sung, P.-W. Chen, C.-J. Yen, M.-R. Shen, C.-H. Chen, K.-J. Tsai, C.-C.K. Lin, Memantine protects against paclitaxel-induced cognitive impairment through modulation of neurogenesis and inflammation in mice, Cancers 13 (2021) 4177, https://doi.org/10.3390/cancers13164177.

[103] Z. Li, J. Zhang, Z. Liu, C.-W. Woo, C.J. Thiele, Downregulation of Bim by brain-derived neurotrophic factor activation of TrkB protects neuroblastoma cells from paclitaxel but not etoposide or cisplatin-induced cell death, Cell Death Differ. 14 (2007) 318–326, https://doi.org/10.1038/sj.cdd.4401983.

[104] X.-Y. Mao, Y.-G. Cao, Z. Ji, H.-H. Zhou, Z.-Q. Liu, H.-L. Sun, Topiramate protects against glutamate excitotoxicity via activating BDNF/TrkB-dependent ERK pathway in rodent hippocampal neurons, Prog. Neuro-Psychopharmacol. Biol. Psychiatry 60 (2015) 11–17, https://doi.org/10.1016/j.pnpbp.2015.01.015.

[105] G.Z. Réus, H.M. Abaleira, S.E. Titus, C.O. Arent, M. Michels, J.R. da Luz, M.A. B. dos Santos, A.S. Carlessi, B.I. Matias, L. Bruchchen, A.V. Steckert, L.B. Ceretta, F. Dal-Pizzol, J. Quevedo, Effects of ketamine administration on the phosphorylation levels of CREB and TrKB and on oxidative damage after infusion of MEK inhibitor, Pharm. Rep. 68 (2016) 177–184, https://doi.org/10.1016/j.pharep.2015.08.010.